

# Composition and correlation of volcanic ash beds of Silurian age from the eastern Baltic

TARMO KIIPLI\*, TOIVO KALLASTE & VIUU NESTOR

Institute of Geology, Tallinn University of Technology, Ehitajate 5, 19086 Tallinn, Estonia

(Received 23 November 2009; accepted 12 February 2010; first published online 21 April 2010)

**Abstract** – Sanidine composition and bulk geochemistry of volcanic ash beds from the East Baltic indicate the subalkaline nature of the volcanism near the margins of the Baltica plate during the Silurian. Several bentonites in the Wenlock include a previously unknown sanidine with 48 to 58 mol % of the Na+Ca component. In contrast to the earlier Telychian volcanism, sodium-rich sanidine occurs in ash beds which originate from relatively moderately evolved dacitic magma. The studied material from two drill cores integrated with previous research enables production of a more complete list of 49 volcanic eruption layers for the lower to middle Wenlock in the East Baltic. This updated list of bentonites characterized by their sanidine compositions forms a good basis for future integrated bio- and chemostratigraphic correlations in northern Europe.

Keywords: K-bentonites, bentonites, geochemistry, Wenlock, Silurian, volcanism, East Baltic.

## 1. Introduction

Northward movement of Baltica and Avalonia continents in early Palaeozoic times reached collision stage with Laurentia in Silurian times (Cocks & Torsvik, 2005). This process caused intensive volcanism in the closing Iapetus Ocean between these continents. Silurian-age igneous rocks are known in the Norwegian Caledonides (Corfu *et al.* 2006), but also in Central Europe (Timmerman, 2008). Sedimentary rocks of Silurian age crop out in Central Estonia and the Baltic Sea islands Saaremaa and Gotland. Fragmentary outcrop areas occur throughout southern-central Sweden and the Oslo Region in Norway. A large continuous subsurface distribution area of Silurian sedimentary rocks occurs from southern Estonia through Latvia and Lithuania to the northeastern part of Poland. Overviews of the occurrence of Silurian altered volcanic ash beds (K-bentonites, bentonites) around the Iapetus palaeo-ocean were published in Bergström *et al.* (1992) and Huff, Bergström & Kolata (2002).

Studies so far of Wenlock bentonites in northern Europe include Cave & Loydell (1998), Batchelor & Jeppsson (1999), Kiipli & Kallaste (2006), Ray (2007) and Kiipli *et al.* (2008a, c). Due to the large number of volcanic eruption layers, and small number of studied sections, data on Wenlock bentonites are still fragmentary and far from satisfactory for reliable correlation of sections using bentonites. Here we present new results from a geochemical study of 37 bentonite layers sampled from the lower and middle Wenlock of the Ventpils D3 and Vidale 263 drill cores (Latvia) and compare these new data with earlier tephrostratigraphic and geochemical studies in the region. The aim of the present study is a geochemical

characterization of lower to middle Wenlock bentonites in the East Baltic and production of a new, more complete list of volcanic ash horizons, that can be used for correlations in future studies in wider areas in northern Europe.

Aspects of the biostratigraphy the Ohesaare core have been published by Kaljo (1970) and Loydell, Kaljo & Männik (1998), the Ventpils D3 core by Gailite, Ulst & Jakovleva (1987) and the Ruhnu 500 core by Pöldvere (2003). The chitinozoans of these cores have been studied by Nestor (1994). The biostratigraphy of the Vidale 263 core has not been previously published.

## 2. Material and methods

Thirty-seven thin bentonites varying in thickness from 0.1 to 6.0 cm (online Appendix at <http://journals.cambridge.org/geo>) were collected from the Ventpils D3 and Vidale 263 cores drilled in West Latvia (Fig. 1). These cores are stored in the Latvian Agency of Environment, Meteorology and Geology. While the host shales are grey, the altered volcanic ashes can be recognized by their yellowish or bluish-grey colour. Biotite phenocrysts visible to the naked eye often confirm the volcanic origin of the bentonites. Very thin volcanic ash beds were sampled together with the host shale, and separation was performed in the laboratory by picking out fragments of different colours. In these cases both volcanic ashes and host shales were analysed.

With the aim of identifying major minerals in the sampled interbeds, randomly oriented bulk samples were analysed by X-ray diffractometry (XRD). An association of illite–smectite and kaolinite as major minerals has been considered to confirm the volcanic origin of the interbeds. More rarely, volcanic ash has been altered to authigenic K-sanidine with minor

\* Author for correspondence: [tarmo.kiipli@gi.ee](mailto:tarmo.kiipli@gi.ee)

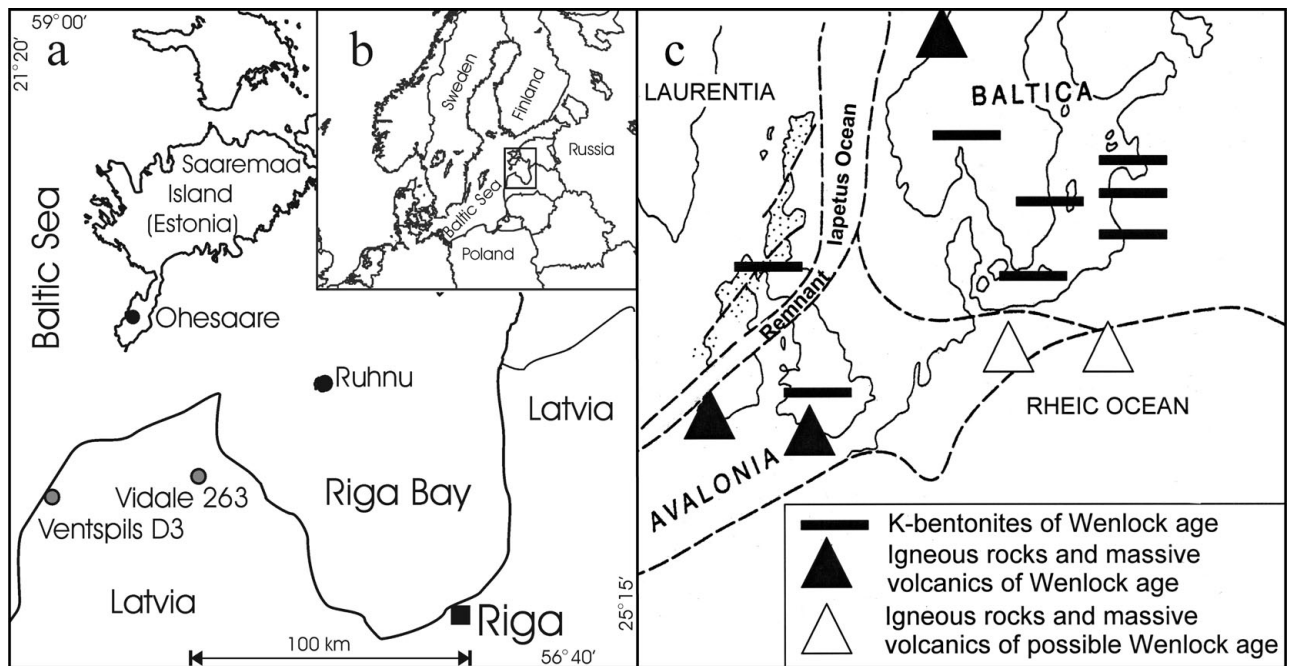


Figure 1. (a) Location of drill holes. Grey rings – sections studied in this work; black rings – sections studied in Kiipli & Kallaste (2006). Wider area (b) with location of studied region. Sketch of Wenlock palaeogeography (c) according to Cave & Loydell (1998) showing colliding Baltica and Laurentia with occurrences of Wenlock age K-bentonites, massive volcanics and igneous rocks of Wenlock age. Stippled area indicates orogenic belts.

illite–smectite and kaolinite (Hints *et al.* 2008). Host shales are composed of a different association of terrigenous minerals including illite, quartz, chlorite and minor K-feldspar.

Magmatic sanidine phenocryst  $(K,Na,Ca)AlSi_3O_8$  composition has proved to be a very useful indicator of particular volcanic eruption layers (bentonites) in earlier Telychian sections from the East Baltic area (Kiipli & Kallaste, 2002; Kallaste & Kiipli, 2006; Kiipli *et al.* 2010). Kastner (1971) demonstrated that sedimentary authigenic feldspars have pure end-member compositions  $KAlSi_3O_8$  or  $NaAlSi_3O_8$  only. Therefore we consider intermediate compositions of the K–Na feldspar (sanidine) as an indication of magmatic origin.

A small percentage of Ca substituted for Na and minor Ba substituted for K in alkali feldspar (Ginibre, Wörner & Kronz, 2004) can influence the position of the sanidine  $20\bar{1}$  reflection. Therefore numerical values of sanidine composition, calculated from that reflection, in reality show the content of the Na+Ca component in mol %. Considering this effect as minor in our previous works (Kiipli & Kallaste, 2002 and other later publications), sanidine composition was expressed in units of Na-component concentration in  $(K,Na)AlSi_3O_8$ . A more accurate expression, Na+Ca component in sanidine, is adopted here. Numerical values herein are still strictly comparable with those in our previous publications.

The phenocrysts were analysed from coarse fractions (0.04–0.1 mm) separated from 2 grams of bentonite. The fraction 0.04–0.1 mm constitutes a very small percentage of the bulk bentonite. Sanidine dominates

among phenocrysts with less abundant biotite and quartz. While biotite occurs often as hexagonal plates, sanidine and quartz are commonly represented by irregular fragments (shards) of the original crystals. Minor apatite and zircon are observed in some layers. Plagioclase phenocrysts, which are commonly the most abundant in silicic magmas, are not preserved in the East Baltic ash beds, since they were most likely dissolved and recrystallized into clay minerals. The  $20\bar{1}$  reflection was measured in a range from  $23.5$  to  $26.0$  ° $2\theta$  using Fe filtered Co  $K\alpha$  radiation. From the position of the  $20\bar{1}$  reflection, the  $(Na,Ca)AlSi_3O_8$  content in  $(K,Na,Ca)AlSi_3O_8$  solid solution (sanidine) was calculated according to Orville (1967). In favourable cases (sharp reflection and low content of authigenic potassium feldspar), the precision of the method was  $\pm 1\%$ . In less favourable cases the precision was  $\pm 2\%$ . Checking of the method by EDS microanalyses in two samples showed reasonable accordance within analytical uncertainty of both methods; in Ventspils 715.4 m EDS analysis showed  $Na_{0.45}Ca_{0.03}K_{0.52}Ba_{0.00}Al_1Si_3O_8$  and XRD showed  $(Na,Ca)_{0.50}(K,Ba)_{0.50}Al_1Si_3O_8$ ; in Ventspils 720.6 m EDS showed  $Na_{0.32}Ca_{0.01}K_{0.65}Ba_{0.02}Al_1Si_3O_8$  and XRD showed  $(Na,Ca)_{0.30}(K,Ba)_{0.70}Al_1Si_3O_8$ . XRD analysis is performed simultaneously on 1000–2000 grains of sanidine and therefore represents average composition of the sample better than EDS microanalysis performed on only some tens of grains. All measured XRD spectra are available in the collections database of the Institute of Geology Tallinn University of Technology at <http://sarv.gi.ee/reference.php?id=1203>.

Many volcanic ash beds show a very wide sanidine reflection which does not permit identification of a particular bed, but nevertheless separates these beds clearly from those with a sharp reflection. Wide reflections indicate heterogeneous composition of the sanidine, caused most probably by presence of the zoned crystals in a source magma. Examples of the measured XRD profiles with curve fitting results from the Wenlock of Latvia are shown in Figure 2.

Samples of sufficient size, at least 8 g, were analysed by the standard X-ray fluorescence (XRF) method from pressed powders for major and trace elements, applying empirical correction coefficients to the measured intensities of spectral lines, at the Institute of Geology Tallinn University of Technology. Precision of the method was mostly better than  $\pm 5\%$  of the concentration and for trace elements in the range 10–30 ppm better than  $\pm 10\%$ . For calibration and quality control, reference materials from France (Govindaraju, 1995) and Estonia (Kiipli *et al.* 2000) were used. Long range accuracy of the method is shown in Kiipli *et al.* (2008b).

### 3. Stratigraphy

In terms of chitinozoan biozonation, the studied interval in the Ventpils D3 and Vidale 263 cores belongs to the *Margachitina margaritana* to *Conochitina subcyatha* biozones (Figs 3, 4). According to Nestor (1994), this interval comprises the lower Sheinwoodian to lower Homerian. In Vidale 263 the *Conochitina tuba*, *Cingulochitina cingulata*, *Eisenackitina spongiosa* and *Conochitina pachycephala* biozones were established (Fig. 3).

## 4. Results

### 4.a. General results

In the studied stratigraphic range (in terms of chitinozoan biozones from *M. margaritana* to *C. subcyatha*), 71 bentonite interbeds occur in four drill cores (Fig. 4). Using the chitinozoan biozonation as a framework and based on the sanidine properties, these bentonites can be grouped into 47 volcanic eruption layers (Table 1). Previously, in the Ohesaare and Ruhnu cores (Kiipli & Kallaste, 2006) only 28 eruption layers were recognized in this interval. In the Vattenfallet exposure on Gotland, a bentonite with a sharp sanidine reflection and 28.5 mol % of Na+Ca-component was found within the upper *K. ranuliformis* conodont Biozone (Kiipli *et al.* 2008a). In Lithuania near the *antennularius/flexilis* graptolite biozone boundary, a bentonite with a wide sanidine reflection and about 26–27 mol % of Na+Ca component was identified (Kiipli *et al.* 2008c). These two bentonites have not been found in Estonian and Latvian sections. Therefore the total volcanic record at the level of present knowledge comprises 49 eruption layers in the studied interval. This list is still provisional, because only eight

correlations are well proved, based on sharp sanidine reflections (Table 1; Figs 4, 5), and nine correlations are less certain, characterized by wide sanidine reflections. Consequently, the larger number of eruption layers is established only in a single section.

Several bentonites are also newly recognized with a previously unknown type of sanidine XRD spectrum indicating the presence of sodium-rich, up to 58 mol %, components in alkali feldspar phenocrysts (Figs 2, 5).

### 4.b. *Margachitina margaritana* Biozone

This interval includes four widespread eruption layers: Aizpute (ID311), Ohesaare (ID210), Luskliint (ID150) and Ireviken (ID127). Depths of these bentonites in the Ohesaare core are 351.7 m, 345.8 m, 342.1 m and 340.8 m, respectively (Fig. 4). Bentonite names and ID numbers are those of Kallaste & Kiipli (2006) and Kiipli *et al.* (2010). The Ohesaare Bentonite and the Ireviken Bentonite are also found in the Ventpils core at depths 792.8 m and 789.2 m, respectively (Table 1; Fig. 4). Additionally, 5 cm above the Ohesaare Bentonite a new eruption layer with a sharp sanidine reflection and 37.4 mol % of Na+Ca component was found. In Vidale not one of these layers was found. A possible reason is poor core recovery in this interval causing destruction of thin soft volcanic ash beds.

### 4.c. *Conochitina mamilla* Biozone

Three bentonites containing sanidine with a very wide reflection occur here. Often these very wide reflections exhibit a specific plateau-like shape with a relatively abrupt fall at the Na-rich end of the spectrum (Fig. 2h). The Ohesaare 323.2 m and Ruhnu 435.84 m beds consist of two layers differing in colour. The first contains sanidine with a plateau-like spectrum and the other sanidine with a sharp reflection with 45–46 mol % of Na+Ca component. In Ventpils 767.15 m and Vidale 709.90 m, only the plateau-like type was found.

The Vidale 703.15 bed, possibly belonging to this biozone, contains sanidine with a sharp reflection.

### 4.d. *Conochitina tuba* Biozone

In the lower part of the biozone, two bentonites with wide sanidine reflections occur in the Ohesaare and Ruhnu sections. In the upper part of the biozone in Ohesaare, four bentonites with sharp sanidine reflections have been found. In Vidale 694.90 m a sharp sanidine reflection was also found, being very similar to the Ohesaare 301.95 m and Ohesaare 301.36 m beds. According to the sampling depth records, the Vidale 694.90 m bentonite must belong to the lower part of the *C. cingulata* Biozone, but this is only 10 cm above the first sample with *C. cingulata*, and small uncertainties in depth interpretations between bentonite researchers and biostratigraphers are possible. We consider the Vidale 694.90 m bed as belonging in the *C. tuba*

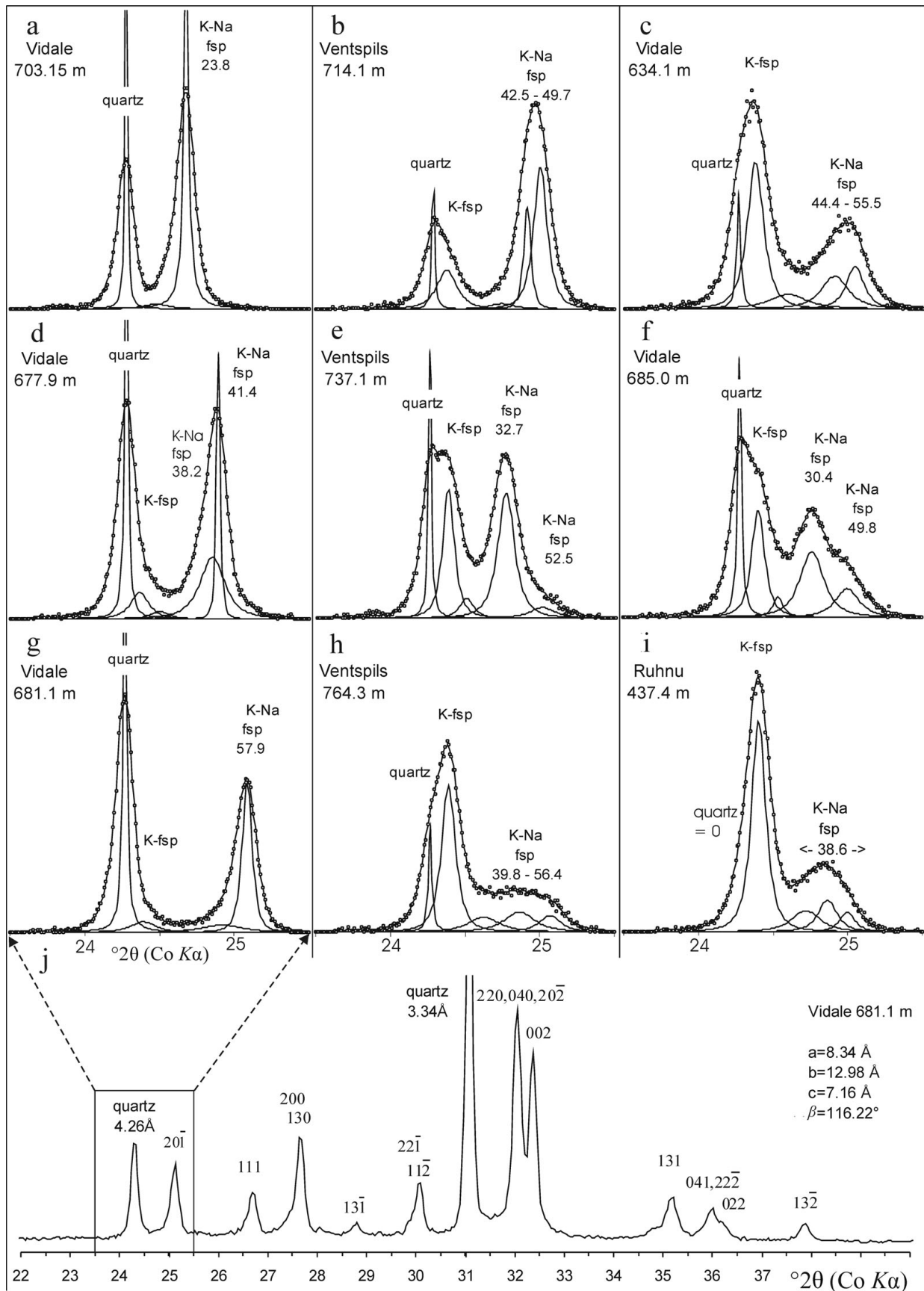


Figure 2. Selected sanidine spectra from studied bentonites. Points mark measured curve, and solid lines reflections of minerals calculated using three, four or five component curve-fitting program; from left to right: quartz, authigenic potassium feldspar (K-fsp) and magmatic K–Na-sanidine (K–Na fsp) described by one, two or three components. Numbers above reflection represent calculated (Na,Ca)AlSi<sub>3</sub>O<sub>8</sub> content (mol %) in sanidine main component. (a–i) Various types of sanidine spectra from 23.5 to 25.5 degrees. (j) Longer XRD pattern of the sanidine from the Vidale core depth 681.1 m.

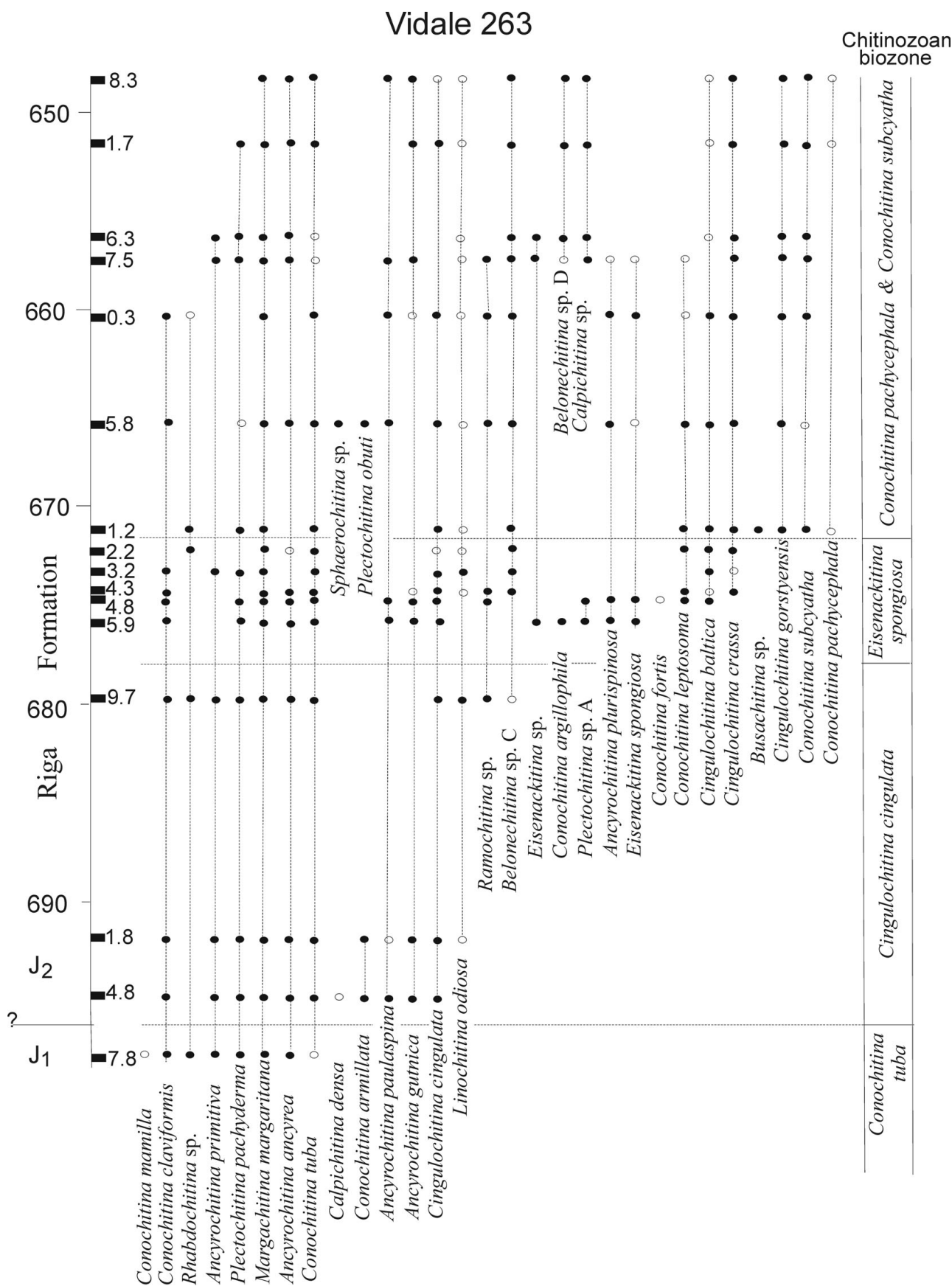


Figure 3. Distribution of chitinozoans in the Vidale 263 core.

Biozone on the basis of a very similar sanidine XRD reflection with bentonites from the upper part of *C. tuba* in Ohesaare.

The step-by-step rise of the Na+Ca-component in sanidine in closely spaced eruption layers starting from Vidale 703.15 m to Ohesaare 300.25 m is remarkable.

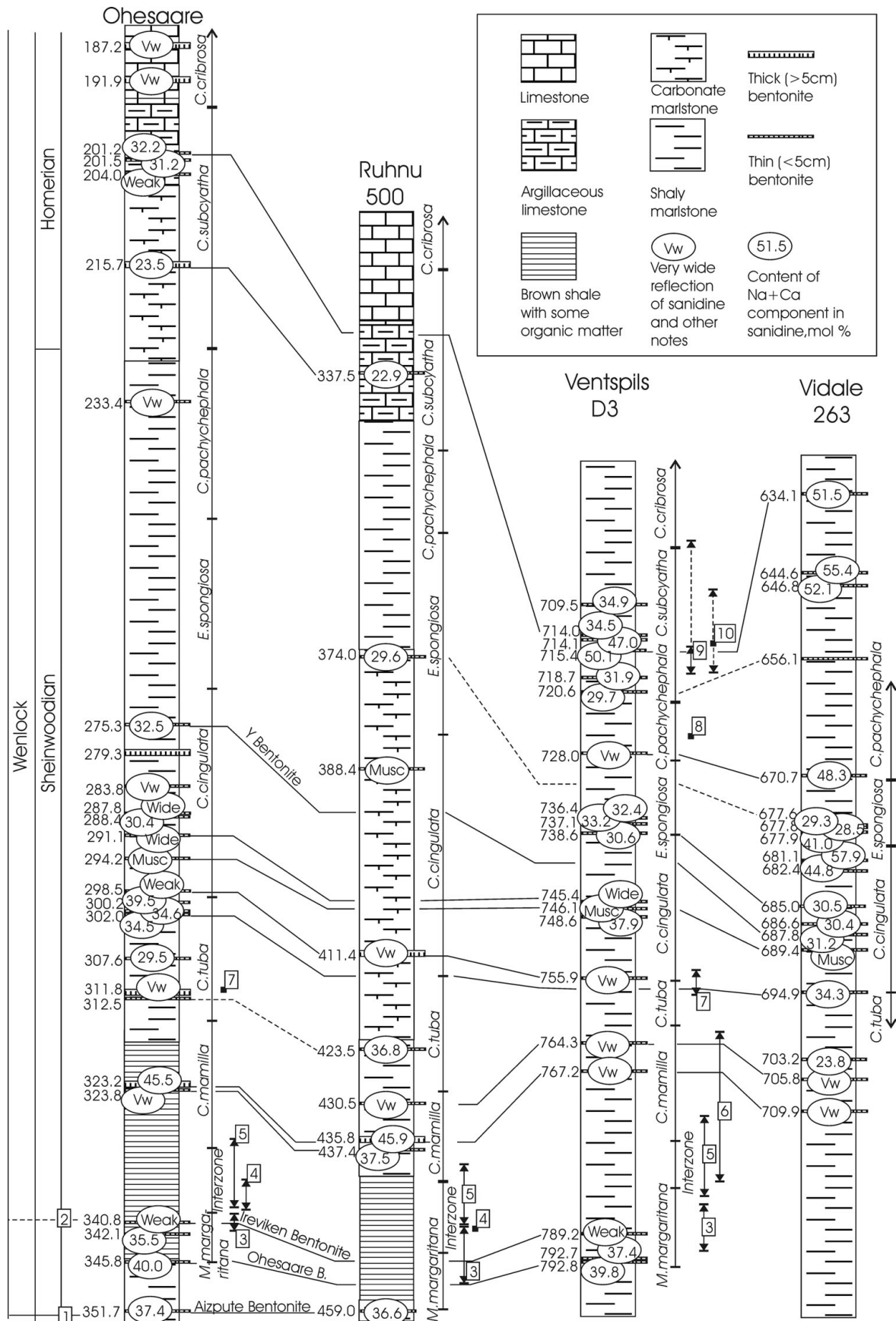


Figure 4. Geological sections of studied drill cores. 1 – traditional Llandovery/Wenlock boundary at the FAD of *Cyrtograptus centrifugus* marked by the Aizpute Bentonite (Martinsson, Bassett & Holland, 1981; Kiipli *et al.* 2010). 2 – Llandovery/Wenlock boundary proposed by Kiipli & Kallaste (2006) and Kiipli *et al.* (2008a) marked by the Ireviken Bentonite. 3–10 – finds of zonal graptolites (Loydell, Kaljo & Männik, 1998; Gailite, Ulst & Jakovleva, 1987; Pöldvere, 2003); 3 – *Cyrtograptus murchisoni*, 4 – *Monograptus firmus*, 5 – *Monograptus riccartonensis*, 6 – *Streptograptus antennularius*, 7 – *Monograptus flexilis*, 8 – *Cyrtograptus radians*, 9 – *Testograptus testis*, 10 – *Cyrtograptus lundgreni*.

Table 1 Occurrence of Wenlock bentonites in the frame of chitinozoan biozonation

Chitinozoan biozones	Ohesaare, depth (m)	Ruhnu, depth (m)	Ventspils, depth (m)	Vidale, depth (m)	Sanidine main component		Biotite
					Peak width, 2 theta	(Na,Ca)AlSi <sub>3</sub> O <sub>8</sub> mol %	
<i>C. subcyata</i>			709.50		0.09	34.9	++
<i>C. subcyata</i>	201.20		714.05		0.13–0.14	32.2–34.5	++
<i>C. subcyata</i>			714.10		0.18	49.8	++
<i>C. subcyata</i>	201.50				0.17	31.2	++
<i>C. subcyata</i>	203.96				Weak		+++
<i>C. subcyata</i>			715.40	634.10	0.23–0.25	50.1–51.5	+
<i>C. subcyata</i>				644.60	0.22	54.1	+
<i>C. subcyata</i>				646.80	0.31	51.3	++
<i>C. subcyata</i>			718.70		Weak		++
<i>C. subcyata</i>	215.70	337.50			0.06–0.07	22.9–23.5	+++
<i>C. subcyata</i>			720.60	656.10	0.09	29.7	++
<i>C. pachycephala</i>	233.44				Very wide		
<i>C. pachycephala</i>			728.05	670.70	Very wide		++
<i>E. spongiosa</i>		374.00		677.60	0.06–0.16	29.3–29.6	++
<i>E. spongiosa</i>				677.75	0.17	28.5	++
<i>E. spongiosa</i>				677.90	0.08	40.9	++
<i>E. spongiosa</i>			736.40		0.27	32.4	+
<i>E. spongiosa</i>			737.10		0.21	33.2	+
<i>C. cingulata</i>				681.10	0.10	57.9	no
<i>C. cingulata</i>				682.40	0.27	44.8	+
<i>C. cingulata</i>		388.40			Weak		M
<i>C. cingulata</i>			738.60	685.00	0.22–0.27	30.5–30.6	++
<i>C. cingulata</i>				686.60	0.30	30.4	+
<i>C. cingulata</i>	275.32			687.80	0.12–0.18	31.2–32.5	+
<i>C. cingulata</i>	283.78				Very wide		+++
<i>C. cingulata</i>	287.85				Wide		no
<i>C. cingulata</i>	288.44				0.11	30.4	++
<i>C. cingulata</i>	291.09		745.40		Wide		+
<i>C. cingulata</i>	294.23		746.10	689.40	Weak		M
<i>C. cingulata</i>			748.60		Weak		no
<i>C. cingulata</i>	298.51	411.45	755.90		Very wide		no
<i>C. tuba</i>	300.25				0.12	39.5	no
<i>C. tuba</i>	301.36				0.06	34.6	++
<i>C. tuba</i>	301.95			694.90	0.08–0.10	34.3–34.5	++
<i>C. tuba</i>	307.61				0.08	29.5	+++
<i>C. tuba</i>	311.80				Very wide		no
<i>C. tuba</i>	312.46	423.50			0.28	36.8	+
<i>C. mamilla</i>				703.15	0.07	23.8	++
<i>C. mamilla</i>		430.50	764.30	705.80	0.22–0.30	48.1–52.3	no
<i>C. mamilla</i>	323.20	435.84	767.15	709.90	0.26–0.34	46.8–47.7	+
<i>C. mamilla</i>	323.21	435.84			0.19–0.20	45.5–45.9	++
<i>C. mamilla</i>	323.85	437.40			Very wide		+
<i>M. margaritana</i>	340.79		789.20		Weak		+++
<i>M. margaritana</i>	342.08				0.24	35.5	no
<i>M. margaritana</i>			792.70		0.13	37.4	+
<i>M. margaritana</i>	345.83		792.75		0.25–0.27	39.8–40.0	+
<i>M. margaritana</i>	351.70				0.08–0.12	36.2–37.8	+

+++ Biotite is abundant; ++ Biotite is rare (10–100 flakes); + Less than 10 flakes; M – muscovite

This may indicate the fractional crystallization and settling of potassium-rich sanidine into the lower parts of a magma chamber.

4.e. *Cingulochitina cingulata* Biozone and lower part of *Eisenackitina spongiosa* Biozone

Most of the approximately thirteen eruption layers in the *C. cingulata* Biozone are characterized by sanidines with wide and very wide spectra, and correlations are therefore hypothetical. In the lower part of the biozone an ash bed containing muscovite can be recognized in the Ohesaare 294.23 m, Ventspils 746.10 m and Vidale 689.40 m beds. Another eruption layer containing muscovite occurs in the upper part of the biozone in the Ruhnu core at a depth of 388.40 m.

Remarkable layers occur in the middle and upper part of the *C. cingulata* Biozone with wide sanidine reflections (Figs 2e–f, 5) requiring five-component fitting of the XRD spectrum (commonly four-component fitting is sufficient). These five fitting profiles (XRD reflections) represent quartz, K-sanidine and three K–Na sanidine components. This type occurs in the Vidale core at depths of 687.80 m, 686.60 m and 685.00 m. In the Ohesaare core this type occurs at a depth 275.32 m. This layer was previously correlated with the Y Bentonite from the Slite quarry on Gotland, Sweden (Kiipli *et al.* 2008a). In the Ventspils core this type of sanidine occurs at a depth of 738.60 m in the *C. cingulata* Biozone and 737.10 m and 736.40 m in the lower part of the *E. spongiosa* Biozone. During sampling of the Ventspils core, we noticed that there

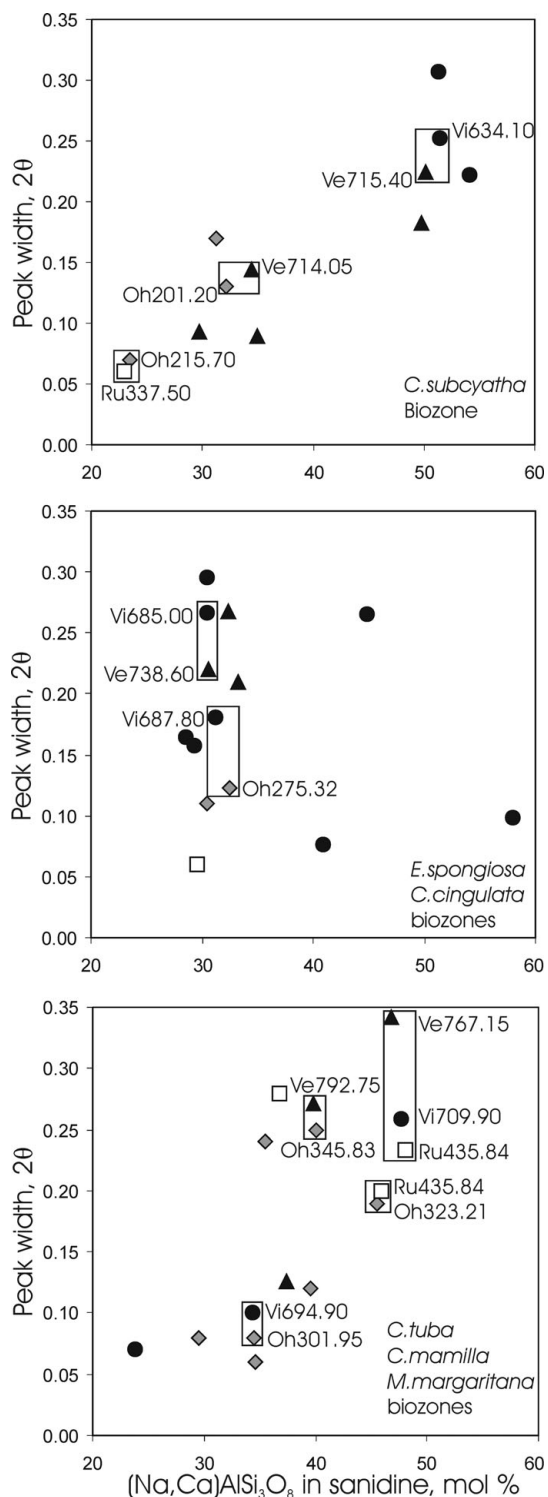


Figure 5. Sanidine composition in the lower and middle Wenlock. Frames join sanidine from correlated ash beds. Many ash beds with sanidine showing wide reflections are not represented here, because the compositions of these sanidines cannot be reliably expressed in numerical values by the method used. Black circles – Vidale (Vi); black triangles – Ventspils (Ve); grey rhombs – Ohesaare (Oh); empty squares – Ruhnu (Ru) section. Numbers represent depths of correlated bentonites (m).

was low recovery of core at this level, and no clearly understandable depth records. Therefore it cannot be excluded that occurrence of some beds of this type in the *E. spongiosa* Biozone can be considered as an

artefact arising from different interpretations of depths. Future studies of more sections must make clear the real number of eruption beds of this type. In Table 1 and online Appendix Table 3, the fourth (main) component of the sanidine exhibiting 30–33 mol % of the Na+Ca-component is reported. The fifth component has lower intensity and contains about 50 mol % ( $\pm 4$  mol %) of the Na+Ca-component.

In addition to the beds with wide sanidine reflections, a few with sharp reflections have also been discovered, for example, in beds from Ohesaare 288.44 m and Vidale 681.10 m. The latter is characterized by an unusually high content of the Na+Ca-component, 57.9 mol % (Fig. 2g).

#### 4.f. *Eisenackitina spongiosa* Biozone

As well as two bentonites containing sanidine with wide reflections in the lower part (see above), we found three bentonites in this biozone in Vidale containing sharp sanidine reflections (Table 1). A bentonite from Ruhnu at 374 m also contains sanidine with a similar Na+Ca-component to that in Vidale 677.60 m, but the reflection is much sharper and this raises some doubt about the correlation of these layers.

#### 4.g. *Conochitina pachycephala* Biozone

At the lower boundary of the biozone an ash bed containing sanidine with a very wide reflection occurs in the Ventspils (728.00 m) and Vidale (670.70 m) cores. In the upper part of the biozone in the Ohesaare (233.40 m) core, another eruption layer occurs with similar sanidine.

#### 4.h. *Conochitina subcyatha* Biozone

In the lower and upper part of this biozone several eruption layers occur with sharp sanidine reflections and 23–35 mol % of the Na+Ca component. In the middle of the biozone in the Ventspils (715.40 m, 714.10 m) and Vidale (646.80 m, 644.60 m, 634.10 m) cores occur bentonites with a wide sanidine reflection and around 50 mol % of the Na+Ca component (Fig. 2b, c). This type of sanidine was not found in previous studies (Kiipli & Kallaste, 2006; Kiipli *et al.* 2008a, c).

#### 4.i. Geochemistry of major components and the discrimination between volcanic ash interbeds and host rock

The host rocks in the Wenlock part of these cores are represented by shales containing 15–30 % of carbonate material. Illite, chlorite, quartz, calcite and dolomite are major minerals in the host shales. Major minerals in the bentonites are kaolinite, illite–smectite, K-feldspar and pyrite. XRF analyses (online Appendix at <http://journals.cambridge.org/geo>) showed unusually high contents of sulphur in bentonites reaching 9 % (Fig. 6a). Host marlstones contain on average only



0.5 % sulphur. Judging from the composition of bentonites showing low sulphur content, altered volcanic ashes contain only about 1–2 % of silicate Fe<sub>2</sub>O<sub>3</sub>. Host shales contain 3–5 % of silicate Fe<sub>2</sub>O<sub>3</sub>. A larger deviation of the bentonite regression line from the pyrite line at higher concentrations is caused by weathering of pyrite and partial removal of sulphur in drill-core boxes during the long storage time (20 years for Vidale 263 and 40 years for the Ventspils D3 core). This is confirmed by the occurrence of jarosite and gypsum reflections on XRD patterns from samples with the highest content of sulphur. The probable reason for the higher content of pyrite in bentonites compared with host shales is that the rapid accumulation of volcanic ash changes the decay of organic matter from oxic on the sea floor to sulphate reducing in the sediment.

Bentonites in the Ventspils and Vidale cores are characterized by a low (1–5 %) K<sub>2</sub>O content in 90 % of the analysed samples and a high (24–35 %) Al<sub>2</sub>O<sub>3</sub> content in 80 % of the samples. The abundance of kaolinite and consequently the low-potassium high-aluminium type of altered volcanic ash beds is typical of Palaeozoic deep shelf environments in the East Baltic (Kiipli *et al.* 2007; Hints *et al.* 2008). This composition means that in this report we favour using the term ‘bentonite’ instead of ‘K-bentonite’, the latter being characterized by much higher (5–12 %) potassium concentrations (Kiipli *et al.* 2008b). High-aluminium kaolinite-rich altered volcanic ash beds found in coal formations are called tonsteins (Bohor & Triplehorn, 1993). In Figure 6b the contents of Al<sub>2</sub>O<sub>3</sub> and K<sub>2</sub>O in the studied samples are recalculated to a pyrite-free composition. The background rock type fields on the chart are composed according to analytical data in Kiipli *et al.* (2008b, d). The host rocks cluster in a clearly different field caused by the higher content of quartz and carbonates. Within the central and southern part of the Baltic Basin between depths 600 and 800 m (studied depth range in Ventspils and Vidale) in bentonites, the content of smectite layers in illite–smectite ranges between 25 and 45 % (Somelar, 2009).

**4.j. Geochemistry of trace elements, interpretation of source magma and tectonic setting**

*4.j.1. General*

Volcanic ash alteration on the seafloor and in sediments leads to the formation of clay minerals. During this process 50 % or more of the original SiO<sub>2</sub> and cations are leached out (Huff, Kolata & Bergström, 1996; Kiipli, Kiipli & Kallaste, 2006). Therefore, easily soluble elements in bentonites cannot be used for interpreting the source magma. In contrast, concentrations of elements of low solubility increase in the forming bentonites. For example, the Al<sub>2</sub>O<sub>3</sub> content in silicic magmatic rocks varies mostly between 10 and 18 %, but in altered volcanic ashes (bentonites) the Al<sub>2</sub>O<sub>3</sub> content is much higher being within a range of 18–36 % (Fig. 6b). Alternatively, immobile trace elements

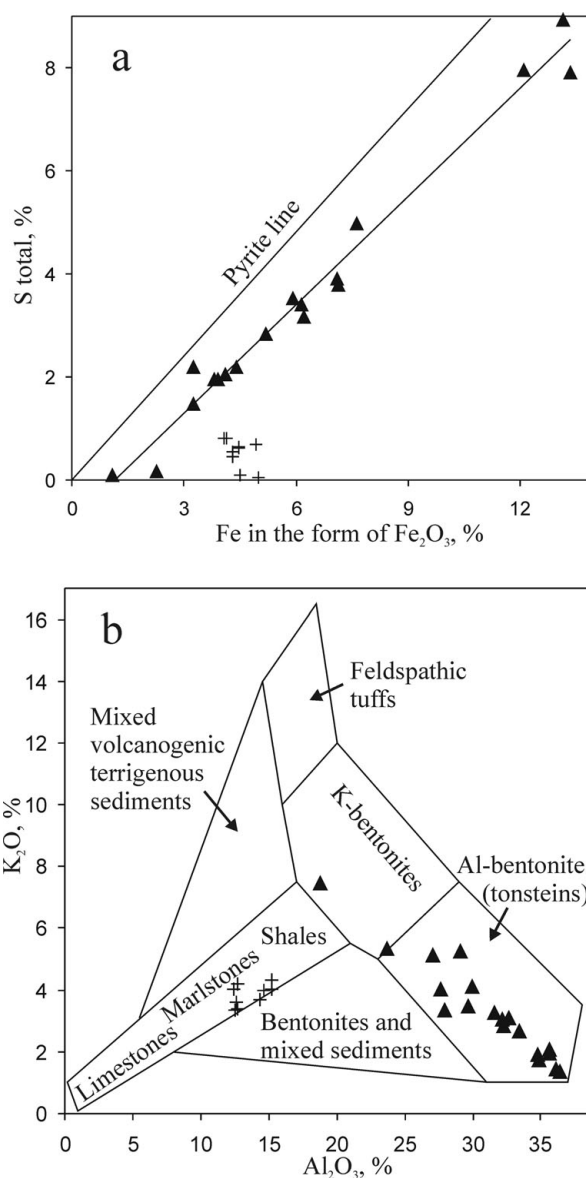


Figure 6. Comparison of major components in altered volcanic ash beds and host shales and marlstones. Black triangles – Wenlock bentonites from the Ventspils D3 and Vidale 263 drill cores. Crosses – host shales from the same cores. Rock fields on (b) are composed using analytical data from Kiipli *et al.* (2008b, d).

(Ti, Zr, Y, Nb, Ce, Ga, Sc) can be used tentatively to interpret initial magma compositions (Winchester & Floyd, 1977). The problem is that concentrations of immobile elements also rise during the formation of clay from volcanic ash. In this paper, following the approach proposed by Kiipli *et al.* (2008d), we are using corrected values for immobile trace elements calculated as follows:

$$I_S = (14/Al_2O_3) \times I_B$$

where I<sub>S</sub> is approximate concentration of immobile trace element in source magma; I<sub>B</sub> is immobile trace element concentration in bentonite; 14 is average content of Al<sub>2</sub>O<sub>3</sub> in silicic magmatic rocks (%),

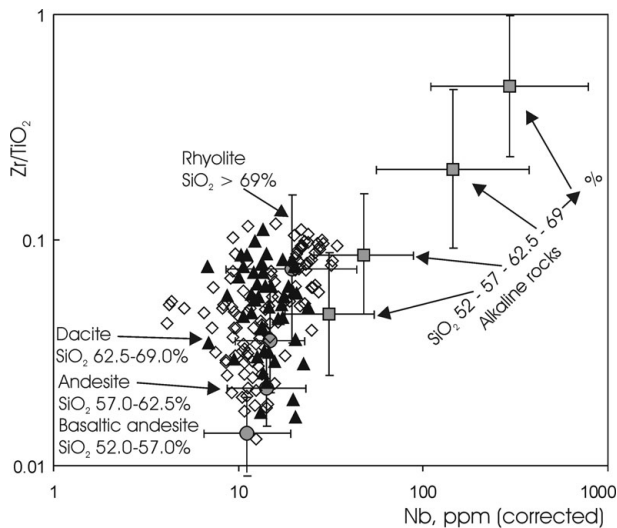


Figure 7. Comparison of Wenlock volcanism (black triangles) and earlier Telychian volcanism (empty rhombs) in the East Baltic with Pliocene to Quaternary volcanism in Italy using the  $Zr/TiO_2$  ratio and Nb. Grey rings represent the geometric mean of the calc-alkaline rocks and grey quadrangles alkaline rocks from Italy. One standard deviation (as a coefficient) is shown by bars. Data from Italian volcanic rocks are from Peccerillo (2005), Telychian bentonites from Kiipli *et al.* (2008d) and Wenlock bentonites in addition to the present study are from Batchelor & Jeppson (1999) and Kiipli *et al.* (2008a, c, d).

(Turekian & Wedepohl, 1961);  $Al_2O_3$  is content of aluminium oxide in bentonite (%).

This calculation gives values on average 50% lower for immobile trace elements than analysed in bentonites, and these values are considered to be closer to the original concentrations. Scaling immobile trace element concentrations back to the supposed initial  $Al_2O_3$  content enables more accurate use of many trace element diagrams. This method enables the use of element ratio diagrams as well as element concentration diagrams for altered volcanic rocks such as bentonites and K-bentonites.

#### 4.j.2. Comparison with Pliocene to Quaternary volcanism in Italy

Intensive volcanic activity during recent geological time in Italy is represented by variable compositions of magmas forming all known volcanic rock types (Peccerillo, 2005). As a hypothesis, the tectonomagmatic environment in the Mediterranean may be considered similar to the environment in a remnant of the Iapetus Ocean between colliding Baltica and Laurentia in Wenlock times.

In Figure 7 the fractionation index, the  $Zr/TiO_2$  ratio, is plotted against Nb concentrations interpreted as an alkalinity index (Winchester & Floyd, 1977; Pearce & Norry, 1979). Using about 1500 analyses of volcanic rocks published by Peccerillo (2005) as a framework (Fig. 7), the source magmas of Wenlock bentonites from the East Baltic can be interpreted as subalkaline, ranging from andesite to rhyolite. Overlapping of

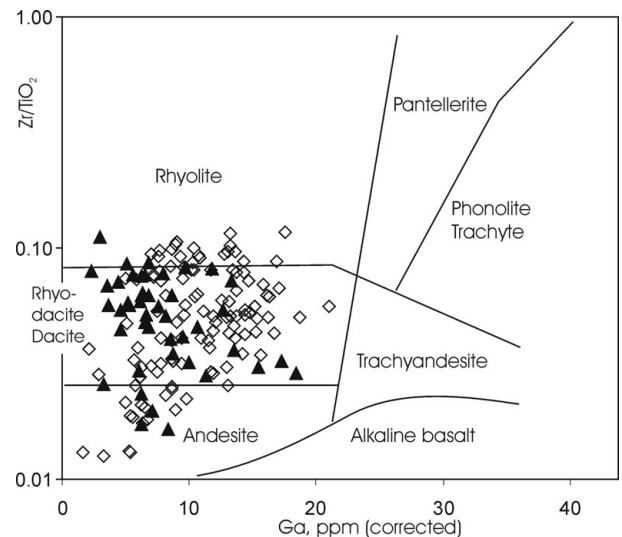


Figure 8. Comparison of Wenlock and Telychian volcanism from the East Baltic on the  $Zr/TiO_2$ -Ga chart according to Winchester & Floyd (1977). Black triangles – Wenlock bentonites; empty rhombs – Telychian bentonites.

compositional ranges in Italian rocks does not exclude some mildly alkaline source magmas for East Baltic bentonites, but also does not prove it. Clearly, strongly alkaline source magmas did not provide the volcanic ash for the East Baltic bentonites. Comparison with earlier Telychian bentonites (Kiipli *et al.* 2008d) reveals essentially overlapping compositional ranges for both ages.

#### 4.j.3. $Zr/TiO_2$ -Ga chart

Winchester & Floyd (1977) proposed Ga in addition to Nb as an alkalinity index for magmatic rocks. Plotting the East Baltic bentonite data onto the framework composed by Winchester & Floyd (1977; Fig. 8) provides confirmation of the interpretation made from comparison with Italian rocks, that most source magmas of East Baltic bentonites were subalkaline. Corrected Ga concentrations are too low for alkaline magmas. Batchelor & Jeppson (1999), based on the composition of apatite phenocrysts, proposed alkaline as well as calc-alkaline magma as a source for the some Wenlock bentonites from Gotland. Wenlock bentonites show, on average, lower corrected Ga concentrations than Telychian ones.

#### 4.j.4. Interpretation of tectonic setting

Using corrected values of Y and Nb on the diagram for granitic rocks proposed by Pearce, Harris & Tindle (1984), these data indicate mostly volcanic arc and syn-collisional tectonic environments for the volcanic sources of the Wenlock bentonites (Fig. 9). A smaller number of points fall in the within-plate granites field.

Wenlock and earlier Telychian volcanism shows a largely overlapping distribution of concentrations with

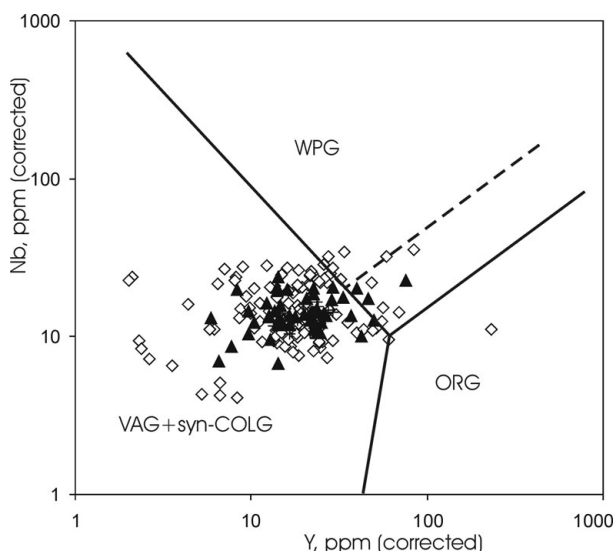


Figure 9. Comparison of Wenlock and Telychian volcanism from the East Baltic on the Y–Nb plot for granitic rocks according to Pearce, Harris & Tindle (1984). Black triangles – Wenlock bentonites; empty rhombs – Telychian bentonites. VAG+syn-COLG – volcanic arc and syn-collisional granites; WPG – within plate granites; ORG – ocean ridge granites.

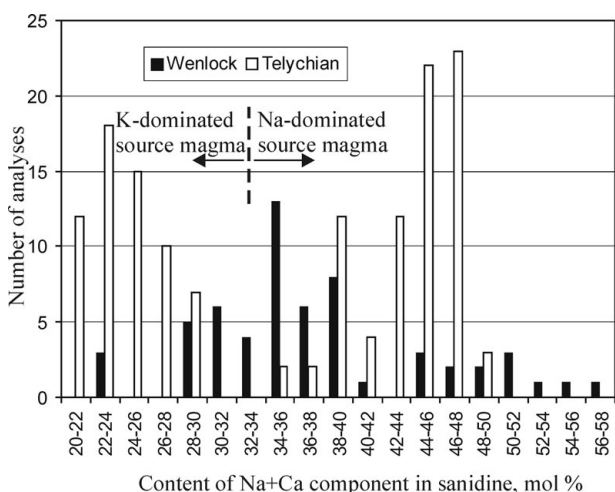


Figure 10. Frequency of the sanidine composition in the East Baltic bentonites. For explanation of separation line between K-dominated and Na-dominated source magma, see text and Figure 12.

the exception of some Telychian bentonites that reveal lower Y values.

4.j.5. Sanidine composition compared in Wenlock and Telychian bentonites

Sanidine composition in Wenlock bentonites shows a bimodal distribution clustering dominantly between 28–40 mol % and 44–58 mol % of the Na+Ca component (Fig. 10). Sanidine in Telychian bentonites also shows a bimodal distribution of composition clustering at 20–30 and 38–48 mol %.

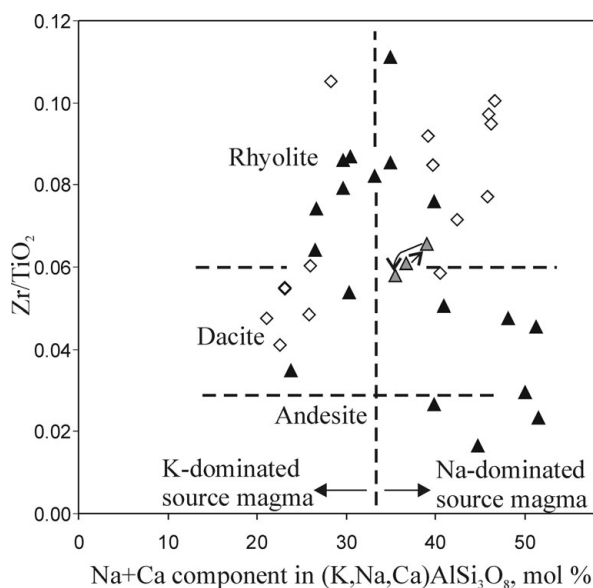


Figure 11. Sanidine composition and Zr/TiO<sub>2</sub> in the East Baltic bentonites with tentative interpretation of source magma. Approximate separation lines between different source magma types are according to Figures 7, 8 and 12. Grey triangles connected with arrows – the lowermost successive bentonites (Aizpute, Ohesaare and Luskint) originated most probably from the same source. Arrows show temporal succession of eruptions.

Comparison of the sanidine compositions with the Zr/TiO<sub>2</sub> ratio (fractionation index) shows that the less evolved dacitic Telychian magmas had more potassic compositions of the sanidine and the highly evolved rhyolitic magmas had more sodic sanidine compositions (Fig. 11). By contrast, later in Wenlock times, less evolved magmas included more sodic sanidine phenocrysts than the highly evolved rhyolitic magmas.

5. Discussion

5.a. Use of sanidine phenocryst composition for geochemical fingerprinting of volcanic eruptions and correlation of sections

High sanidine forms in magma chambers during cooling at high temperatures and is a metastable mineral at Earth surface temperatures (Gill, 1996). After the fast cooling during volcanic eruption, recrystallization of the mineral slows down significantly and has not proceeded much in the East Baltic area, even during the 400 Ma from the Silurian to the present day. This may not be the case everywhere. For example, attempts to analyse sanidine by XRD from the Silurian bentonites of the Oslo region (Norway) correlated by trace elements with bentonites containing sanidine in Estonia (Kiipli *et al.* 2001) did not reveal measurable reflections. Evidently the rocks were heated too much during Caledonian orogenesis or Permian magmatism. Another reason for the lack of sanidine may be a highly chemically reactive environment in some organic rich black shales, for example, in Bornholm, where we also could not find sanidine by XRD. Sanidine may already have been absent in source magma. The precise

causes of a lack of sanidine in particular cases are unknown and must be the topic of future studies. Our present knowledge indicates that XRD measurements of the sanidine composition can be used successfully for geochemical fingerprinting of volcanic ash layers in Estonia, Latvia, Lithuania and Gotland (Sweden). This method can probably also be used in some areas of the mainland of Sweden, as suggested by dating of the Ordovician bentonite from Kinnekulle (southern Sweden) by the K–Ar method using sanidine (Byström-Asklund, Baadsgaard & Folinsbee, 1961).

For establishing correlations of sections by chemical and/or mineralogical fingerprinting of the volcanic ash beds in Palaeozoic sections, two approaches can be used:

(1) Analysing as many geochemical and mineralogical parameters as possible with the aim of finding the unique signature of the particular eruption layer. This approach was used by Bergström *et al.* (1995), Hetherington, Nakrem & Batchelor (2004), Batchelor (2009) and Inanli, Huff & Bergström (2009). Searching for the unique fingerprint is certainly important, but is time consuming and expensive work, and cannot be easily done for a large number of ash beds. This method is well applicable where a few eruption layers occur in sections.

(2) Another approach, analysing with maximum possible accuracy only a single significant parameter, is preferable in sections containing a large number of ash beds (Kiipli *et al.* 2010). The problem is that in this case the same composition (sanidine composition in our study) can occur repetitively in a section. For example, sharp sanidine reflections with a similar content of the Na+Ca component between 28 and 32 mol % occur in the East Baltic Silurian in 12 eruption layers (Kiipli & Kallaste, 2006; Kiipli *et al.* 2010; present study). As the East Baltic Silurian contains more than 100 established volcanic eruption layers, determination of the sanidine composition restricts possible variants for correlation considerably. Additional constraints can be obtained from the biostratigraphical information. Analysing all occurring layers for a single primary magmatic signature with very precise methods enables establishment of a unique succession of many eruptions. The unique temporal succession of several volcanic ash beds can be used, together with biostratigraphy, for correlation of sections even when the analysed parameter shows the same value in several ash beds.

##### 5.b. Integrated petrogenetic interpretation and possible location of source volcanoes

Analysis of immobile trace elements has enabled a provisional estimate of the source magma of the Wenlock bentonites as being subalkaline, ranging from dacite to rhyolite, originating in volcanic arc and syncollisional tectonic settings. Andesite as a source magma indicated by some low Zr/TiO<sub>2</sub> ratios is less probable, because East Baltic Silurian volcanic ashes

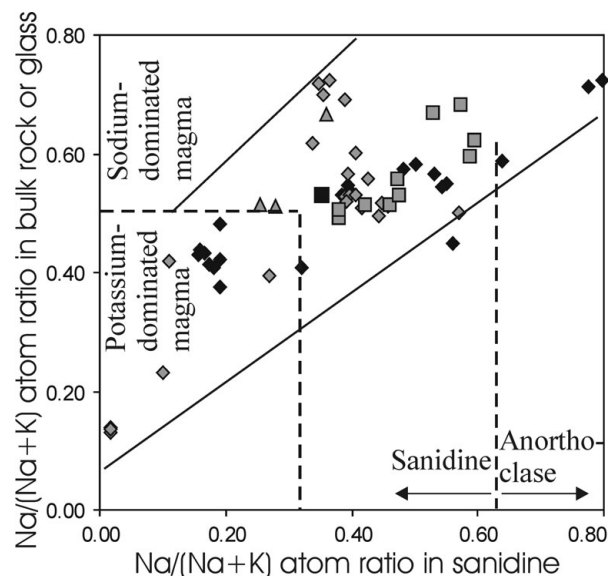


Figure 12. Comparison of the Na/(Na+K) atom ratio in sanidine and coexisting volcanic glass or whole rock. Black – comparison with glass; grey – comparison with whole rock. Rhombs – alkaline rocks; squares – rhyolites; triangles – dacites. Data sources: Anderson, Davis & Lu (2000); Basu & Vitaliano (1976); Carmichael (1967); Chesner (1998); Christiansen (2001); Gaeta (1998); Henry, Price & Smyth (1988); Landi, Bertagnini & Rosi (1999); Maughan *et al.* (2002); Macdonald, Rogers & Tindle (2007); McHenry (2009); Morgan *et al.* (2006); Pappalardo, Ottolini & Mastrolorenzo (2008); Sacchi *et al.* (2005); Smith (1974, pp. 47, 50); Zellmer & Clavero (2006).

commonly contain sanidine as a major phenocryst. In recent andesites, sanidine occurs only rarely as a minor phenocryst (Winter, 2001, p. 303).

Analysis of sanidine composition provides an additional tentative possibility of estimating the potassium/sodium ratio in source magmas. When temperature decreases in a binary NaAlSi<sub>3</sub>O<sub>8</sub>–KAlSi<sub>3</sub>O<sub>8</sub> system, the first crystallizing phase is a potassium-rich sanidine, followed later by a more sodic one (Bowen & Tuttle, 1950). Real magmas are multicomponent systems and crystallization is more complicated. However, empirical comparison of sanidine composition with coexisting volcanic glass and whole rock shows, although strongly scattered, the same relationship (Fig. 12). Pyroclastic sanidine in the East Baltic Silurian forms commonly only a small percentage of the bentonite, indicating that eruptions occurred at the initial stages of sanidine crystallization. Therefore we may suppose higher Na/K ratios in source magma than in sanidine. Based on Figure 12, we can deduce that bentonites containing sanidine with less than approximately 33 mol % of Na+Ca component probably crystallized from potassium-dominated magma and those with more sodium-rich sanidine from the magma where sodium dominates over potassium.

Intrusive rocks of Wenlock age are known from the Scandinavian Caledonides in South Central Norway around Trondheim (Corfu *et al.* 2006). Massive meta-volcanic rocks of Silurian age occur in the Northern Phyllite Zone in Germany (Timmerman, 2008) and in

the Holy Cross mountains in Poland (Krawczyk, 2008). Therefore at the level of present knowledge, volcanic sources for the East Baltic bentonites of Wenlock age could have been in a collision zone between Baltica and Laurentia or in the Central European Caledonides. Mapping of the underlying Telychian and overlying upper Wenlock volcanic ash layers indicated an origin from the Iapetus palaeo-ocean (Kiipli *et al.* 2008a, b, c, d). To enable composition of volcanic ash distribution maps, the lower–middle Wenlock bentonites need to be studied in a wider area in the future.

## 6. Conclusions

Study of sanidine in the lower and middle Wenlock part of the Ventpils D3 and Vidale 263 drill cores reveals about 20 previously unknown eruption layers and gives, in combination with the formerly studied Ohesaare and Ruhnu cores, the most complete list available at this time of volcanic beds for the East Baltic area constrained by the chitinozoan biozonation. XRD measurements revealed several new types of sanidine spectra, in particular, samples with a high Na+Ca (48–58 mol %) content. Sanidine in the studied part of the Wenlock in the East Baltic is of variable composition, having excellent potential for geochemical fingerprinting of volcanic eruption layers.

Immobile trace elements and the sanidine composition indicate subalkaline volcanism generated in volcanic arc and syncollisional tectonic environments. Sanidine composition suggests that both potassium- and sodium-dominated source magmas occurred in the Silurian at the margins of the Baltica plate.

**Acknowledgements.** This study is a contribution to the Estonian Science Foundation grant 7605 and target financing projects SF0140016s09 and SF0140020s08. We thank A. Murnieks, R. Pomeranceva and R. Einasto for kindly helping in sampling in the Latvian Agency of Environment, Meteorology and Geology, the late K. Orlova for XRF analyses, D. K. Loydell for correcting language and two anonymous referees for help.

## References

ANDERSON, A. T., DAVIS, A. M. & LU, F. 2000. Evolution of Bishop Tuff rhyolitic magma based on melt and magnetite inclusions and zoned phenocrysts. *Journal of Petrology* **41**, 449–73.

BASU, A. & VITALIANO, C. J. 1976. Sanidine from the Mesa Falls Tuff, Ashton Idaho. *American Mineralogist* **61**, 405–8.

BATCHELOR, R. A. 2009 (for 2008). Geochemical “Golden Spike” for Lower Palaeozoic metabentonites. *Earth and Environmental Science Transactions of the Royal Society of Edinburgh* **99**, 177–87.

BATCHELOR, R. A. & JEPPESSON, L. 1999. Wenlock metabentonites from Gotland, Sweden: geochemistry, sources and potential as chemostratigraphic markers. *Geological Magazine* **136**, 661–9.

BERGSTRÖM, S. M., HUFF, W. D., KOLATA, D. R. & BAUERT, H. 1995. Nomenclature, stratigraphy, chemical fingerprinting and areal distribution of some Middle

Ordovician K-bentonites in Baltoscandia. *GFF* **117**, 1–13.

BERGSTRÖM, S. M., HUFF, W. D., KOLATA, D. R. & KALJO, D. 1992. Silurian K-bentonites in the Iapetus Region: A preliminary event-stratigraphic and tectonomagmatic assessment. *GFF* **114**, 327–34.

BOHOR, B. F. & TRIPLEHORN, D. M. 1993. Tonsteins: altered volcanic ash layers in coal-bearing sequences. *Geological Society of America Special Paper* **285**, 1–44.

BOWEN, N. L. & TUTTLE, O. F. 1950. The system NaAlSi<sub>3</sub>O<sub>8</sub>–KAlSi<sub>3</sub>O<sub>8</sub>–H<sub>2</sub>O. *Journal of Geology* **58**, 489–511.

BYSTRÖM-ASKLUND, A. M., BAADSGAARD, H. & FOLINSBEE, R. E. 1961. K/Ar age of biotite, sanidine and illite from Middle Ordovician bentonites at Kinnekulle Sweden. *Geologiska Föreningens i Stockholm Förhandlingar* **83**, 92–6.

CARMICHAEL, I. S. E. 1967. The mineralogy and petrology of the volcanic rocks from the Leucite Hills, Wyoming. *Contributions to Mineralogy and Petrology* **15**, 24–66.

CAVE, R. & LOYDELL, D. K. 1998. Wenlock volcanism in the Welsh Basin. *Geological Journal* **33**, 107–20.

CHESNER, C. A. 1998. Petrogenesis of the Toba Tuffs, Sumatra, Indonesia. *Journal of Petrology* **39**, 397–438.

CHRISTIANSEN, R. L. 2001. The Quaternary and Pliocene Yellowstone Plateau Volcanic Field of Wyoming, Idaho, and Montana. *US Geological Survey Professional Paper* **729-G**, 1–159.

COCKS, L. R. M. & TORSVIK, T. H. 2005. Baltica from the late Precambrian to the mid-Palaeozoic times: The gain and loss of terrain's identity. *Earth-Science Reviews* **72**, 39–66.

CORFU, F., TORSVIK, T. H., ANDERSEN, T. B., ASHWAL, L. D., RAMSAY, D. M. & ROBERTS, R. J. 2006. Early Silurian mafic–ultramafic and granitic plutonism in contemporaneous flysch, Magerøy, northern Norway: U–Pb ages and regional significance. *Journal of the Geological Society, London* **163**, 291–301.

GAETA, M. 1998. Petrogenetic implications of Ba-sanidine in the Lionato Tuff, Italy. *Mineralogical Magazine* **62**, 697–701.

GAILITE, L. K., ULST, R. J. & JAKOVLEVA, V. I. 1987. *Stratotype and type sections of the Silurian of Latvia*. Riga: Zinatne, 183 pp.

GILL, R. 1996. *Chemical Fundamentals of Geology*. London: Chapman & Hall, 290 pp.

GINIBRE, C., WÖRNER, G. & KRONZ, A. 2004. Structure and dynamics of the Laacher See magma chamber (Eifel, Germany) from major and trace element zoning in sanidine: a cathodoluminescence and electron microprobe study. *Journal of Petrology* **45**, 2197–223.

GOVINDARAJU, K. 1995. 1995 working values with confidence limits for twenty six CRPG, ANRT and IWG-GIT geostandards. *Geostandards Newsletter* **19**, Special Issue, 1–32.

HENRY, C. D., PRICE, J. G. & SMYTH, R. C. 1988. Chemical and thermal zonation in a mildly alkaline magma system Infiernito Caldera, Trans-Pecos Texas. *Contributions to Mineralogy and Petrology* **98**, 194–211.

HETHERINGTON, C. J., NAKREM, H. A., & BATCHELOR, R. A. 2004. The Bjørntvet metabentonite: A new correlation tool for the Silurian of the southwest Oslo Region. *Norwegian Journal of Geology* **84**, 239–50.

HINTS, R., KIRSIMÄE, K., SOMELAR, P., KALLASTE, T. & KIIPLI, T. 2008. Multiphase Silurian bentonites in the Baltic Palaeobasin. *Sedimentary Geology* **209**, 69–79.

HUFF, W. D., BERGSTRÖM, S. M. & KOLATA, D. R. 2002. Silurian K-bentonites of the Dnestr basin, Podolia,

- Ukraine. *Journal of the Geological Society, London* **157**, 493–504.
- HUFF, W. D., KOLATA, D. R. & BERGSTRÖM, S. M. 1996. Large-magnitude Middle Ordovician volcanic ash falls in North America and Europe: dimensions, emplacement and post-emplacement characteristics. *Journal of Volcanology and Geothermal Research* **73**, 285–301.
- INANLI, F. Ö., HUFF, W. D. & BERGSTRÖM, S. M. 2009. The Lower Silurian (Llandovery) Osmundsberg K-bentonite in Baltoscandia and the British Isles: Chemical fingerprinting and regional correlation. *GFF* **131**, 269–79.
- KALJO, D. (ed.) 1970. *Silurian of Estonia*. Tallinn: Valgus, 343 pp.
- KALLASTE, T. & KIIPLI, T. 2006. New correlations of Telychian bentonites in Estonia. *Proceedings of the Estonian Academy of Sciences, Geology* **55**, 241–51.
- KASTNER, M. 1971. Authigenic feldspars in carbonate rocks. *American Mineralogist* **56**, 1403–42.
- KIIPLI, E., KIIPLI, T. & KALLASTE, T. 2006. Identification of the O-bentonite in the deep shelf sections with implication on stratigraphy and lithofacies, East Baltic Silurian. *GFF* **128**, 255–60.
- KIIPLI, T., BATCHELOR, R. A., BERNAL, J. P., COWING, C., HAGEL-BRUNNSTROM, M., INGHAM, M. N., JOHNSON, D., KIVISILLA, J., KNAACK, C., KUMP, P., LOZANO, R., MICHIELS, D., ORLOVA, K., PIRRUS, E., ROUSSEAU, R. M., RUZICKA, J., SANDSTROM, H. & WILLIS, J. P. 2000. Seven sedimentary rock reference samples from Estonia. *Oil Shale* **17**, 215–23.
- KIIPLI, T., JEPSSON, L., KALLASTE, T. & SÖDERLUND, U. 2008a. Correlation of Silurian bentonites from Gotland and the East Baltic using sanidine phenocryst composition, and biostratigraphical consequences. *Journal of the Geological Society, London* **165**, 211–20.
- KIIPLI, T. & KALLASTE, T. 2002. Correlation of Telychian sections from shallow to deep sea facies in Estonia and Latvia based on the sanidine composition of bentonites. *Proceedings of the Estonian Academy of Sciences, Geology* **51**, 143–56.
- KIIPLI, T. & KALLASTE, T. 2006. Wenlock and uppermost Llandovery bentonites as stratigraphic markers in Estonia, Latvia and Sweden. *GFF* **128**, 139–46.
- KIIPLI, T., KALLASTE, T., NESTOR, V. & LOYDELL, D. K. 2010. Integrated Telychian (Silurian) K-bentonite chemostratigraphy and biostratigraphy in Estonia and Latvia. *Lethaia* **43**, 32–44.
- KIIPLI, T., KIIPLI, E., KALLASTE, T., HINTS, R., SOMELAR, P. & KIRSIMÄE, K. 2007. Altered volcanic ash as an indicator of marine environment, reflecting pH and sedimentation rate – example from the Ordovician Kinnekulle bed of Baltoscandia. *Clays and Clay Minerals* **55**, 177–88.
- KIIPLI, T., MÄNNIK, P., BATCHELOR, R. A., KIIPLI, E., KALLASTE, T. & PERENS, H. 2001. Correlation of Telychian (Silurian) altered volcanic ash beds in Estonia, Sweden and Norway. *Norwegian Journal of Geology* **81**, 179–93.
- KIIPLI, T., ORLOVA, K., KIIPLI, E. & KALLASTE, T. 2008b. Use of immobile trace elements for the correlation of Telychian bentonites on Saaremaa Island, Estonia, and mapping of volcanic ash clouds. *Estonian Journal of Earth Sciences* **57**, 39–52.
- KIIPLI, T., RADZEVICIUS, S., KALLASTE, T., MOTUZA, V., JEPSSON, L. & WICKSRÖM, L. 2008c. Wenlock bentonites in Lithuania and correlation with bentonites from sections in Estonia, Sweden and Norway. *GFF* **130**, 203–10.
- KIIPLI, T., SOESOO, A., KALLASTE, T. & KIIPLI, E. 2008d. Geochemistry of Telychian (Silurian) K-bentonites in Estonia and Latvia. *Journal of Volcanology and Geothermal Research* **171**, 45–58.
- KRAWCZYK, CH. M., MCCANN, T., COCKS, L. R. M., ENGLAND, R. W., MCBRIDE, J. H. & WYBRANIEC, S. 2008. Caledonian tectonics. In *The Geology of Central Europe. Volume 1: Precambrian and Palaeozoic* (ed. T. McCann), pp. 303–81. London: Geological Society.
- LANDI, P., BERTAGNINI, A. & ROSI, M. 1999. Chemical zoning and crystallization mechanisms in the magma chamber of the Pomici di Base plinian eruption of Somma-Vesuvius (Italy). *Contributions to Mineralogy and Petrology* **135**, 179–97.
- LOYDELL, D. K., KALJO, D. & MÄNNIK, P. 1998. Integrated biostratigraphy of the lower Silurian of the Ohesaare core, Saaremaa, Estonia. *Geological Magazine* **135**, 769–83.
- MACDONALD, R., ROGERS, N. W. & TINDLE, A. G. 2007. Distribution of germanium between phenocrysts and melt in peralkaline rhyolites from the Kenia Rift Valley. *Mineralogical Magazine* **71**, 703–13.
- MARTINSSON, A., BASSETT, M. G. & HOLLAND, C. H. 1981. Ratification of Standard Chronostratigraphical Divisions and Stratotypes for the Silurian System. *Lethaia* **14**, 168.
- MAUGHAN, L. L., CHRISTIANSEN, E. H., BEST, M. G., GROMME, C. S., DEINO, A. L. & TINGEY, T. G. 2002. The Oligocene Lund Tuff, Great Basin, USA: a very large volume monotonous intermediate. *Journal of Volcanology and Geothermal Research* **113**, 129–57.
- MCHENRY, L. J. 2009. Element mobility during zeolitic and argillitic alteration of volcanic ash in a closed basin lacustrine environment: Case study Olduvai Gorge, Tanzania. *Chemical Geology* **265**, 540–52.
- MORGAN, D. J., BLAKE, S., RODGER, N. W., DE VIVO, B., ROLANDI, G. & DAVIDSON, J. P. 2006. Magma chamber recharge at Vesuvius in the century prior to the eruption of A.D. 79. *Geology* **34**, 845–8.
- NESTOR, V. 1994. Early Silurian chitinozoans in Estonia and North Latvia. *Academia* **4**, 1–163.
- ORVILLE, P. M. 1967. Unit cell parameters of the microcline-low albite and the sanidine-high albite solid solution series. *American Mineralogist* **52**, 55–86.
- PAPPALARDO, L., OTTOLINI, L. & MASTROLORENZO, G. 2008. The Campanian Ignimbrite (southern Italy) geochemical zoning: insight on the generation of a super-eruption from catastrophic differentiation and fast withdrawal. *Contributions to Mineralogy and Petrology* **156**, 1–26.
- PEARCE, J. A., HARRIS, N. B. W. & TINDLE, A. G. 1984. Trace element discrimination diagrams for the tectonic interpretation of granitic rocks. *Journal of Petrology* **25**, 956–83.
- PEARCE, J. A. & NORRY, M. J. 1979. Petrogenetic implications of Ti, Zr, Y, and Nb variations in volcanic rocks. *Contributions to Mineralogy and Petrology* **69**, 33–47.
- PECCERILLO, A. 2005. *Plio-Quaternary Volcanism in Italy. Petrology, Geochemistry, Geodynamics*. Berlin, Heidelberg, New York: Springer, 365 pp.
- PÖLDVERE, A. (ed.) 2003. Ruhnü (500) drill core, Estonian Geological Sections. *Geological Survey of Estonia Bulletin* **5**, 1–76.
- RAY, D. C. 2007. The correlation of Lower Wenlock Series (Silurian) bentonites from the Lower Hill Farm and

- Eastnor Park boreholes, Midland Platform, England. *Proceedings of the Geologists' Association* **118**, 175–85.
- SACCHI, M., INSINGA, D., MILIA, A., MOLISSO, F., RASPINI, A., TORRENTE, M. M. & CONFORTI, A. 2005. Stratigraphic signature of the Vesuvius 79 AD event of the Sarno prodelta system, Naples Bay. *Marine Geology* **222–223**, 443–69.
- SMITH, J. V. 1974. *Feldspar Minerals 2, Chemical and Textural Properties*. Berlin, Heidelberg, New York: Springer-Verlag, 690 pp.
- SOMELAR, P. 2009. *Illitization of K-bentonites in the Baltic Basin*. *Dissertationes Geologicae Universitatis Tartuensis* **25**, Tartu University Press, pp. 1–118. Published thesis.
- TIMMERMAN, M. J. 2008. Palaeozoic magmatism. In *The Geology of Central Europe. Volume 1: Precambrian and Palaeozoic* (ed. T. McCann), pp. 665–748. London: Geological Society.
- TUREKIAN, K. K. & WEDEPOHL, K. H. 1961. Distribution of the elements in some major units of the Earth's crust. *Geological Society of America Bulletin* **72**, 175–91.
- WINCHESTER, J. A. & FLOYD, P. A. 1977. Geochemical discrimination of different magma series and their differentiation products using immobile elements. *Chemical Geology* **20**, 325–43.
- WINTER, J. D. 2001. *An Introduction to Igneous and Metamorphic Petrology*. Prentice Hall, 697 pp.
- ZELLMER, G. F. & CLAVERO, J. E. 2006. Using trace element correlation patterns to decipher a sanidine crystal growth chronology: An example from Taapaca volcano, Central Andes. *Journal of Volcanology and Geothermal Research* **156**, 291–301.